Polar lows - A challenge for predicting extreme polar weather

Trond Iversen

ECMWF, Shinfield Park, Reading RG2 9AX, United Kingdom
and MET Norway, P.O.Box 43,Blindern, 0313 Oslo Norway
trond.iversen@met.no

with substantial contribution by:

Linus Magnusson (*ECMWF*), **Alex Deckmyn** (*KMI, Belgium*), **Andrew Singleton, Harold McInnes, Inger-Lise Frogner, Jørn Kristiansen, Gunnar Noer, Hanneke Luijting** (*MET, Norway*), **Kai Sattler** (*DMI, Denmark*)

1. Introduction

1.1. Synoptics

Polar lows (hereafter denoted PLs) belong to a class of meso- and sub-synoptic scale cyclones that form during winter and spring over ocean areas without sea-ice at high latitudes, see Figure 1. The main features of PLs in the Barents and Norwegian Sea was described by Wilhelmsen (1985), based on the experience of a duty forecaster exploiting the sparse regular synoptic observations and the descriptions by people that had been hit by the phenomenon at sea. There are several different types of PLs, and Rasmussen and Turner (2003) give a generalized description of a PL as *a small, but fairly intense maritime cyclone that forms poleward of the main baroclinic zone with a horizontal scale approximately between 200 and 1000 km and surface winds near or above gale force.* Even though the term "fairly intense" may seem to imply low levels of hazardous impacts, it should be emphasized that the associated weather can be dangerous due to a combination of moderate to strong winds with high intensity snowfall, high waves, and freezing sea-spray. Furthermore, their fast development on sub-synoptic scales in areas with very few traditional observations put additional risks to any human activity exposed to these conditions. Local fishermen and their families have been aware of the considerable risk of sudden hazardous weather developments in the open waters
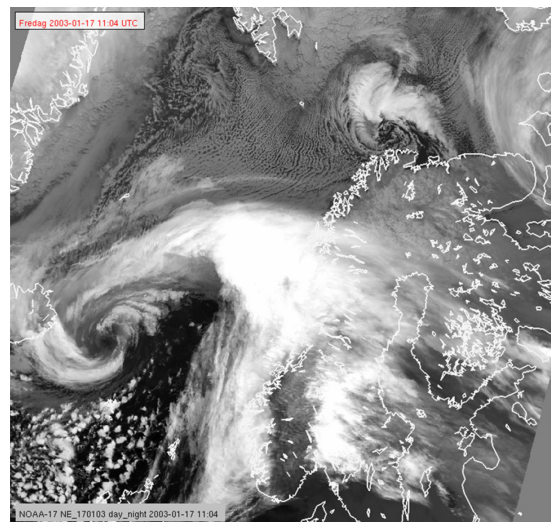

Figure 1: Infrared satellite picture valid at 17.01.2003 11:04 UTC (NOAA-17), illustrating the different appearance between a developed frontal cyclone and a mature

outside Northern Norway for centuries.

As documented by Kristjánsson et al (2011) in the summary paper on the Norwegian IPY-Thorpex project, there has also been scientific awareness of this type of weather situations for more than a century. Early on Vilhelm Bjerknes even associated its physics with the anomalously high temperature with ice-free ocean surfaces far into the Arctic. When infrared satellite imagery from polar orbiting satellites became available to weather forecasters in the 1960s the adverse weather was better identified as small-scale and short-lived cyclones which formed over polar seas. Early on they were called instability lows due to the strong influence of deep convection when cold air is advected over the much warmer open ocean (Rabbe, 1975; Økland 1977). The term "polar lows" has later been commonly used, although "Arctic hurricanes" has also been proposed (Emanuel and Rotunno, 1989) due to the analogy to tropical cyclones.

The combination of fast developing, small-scale systems in areas with little observations has long been a tough challenge for weather forecasters on duty. In the modern era of numerical weather forecasting and advanced data-assimilation forecasting PLs still appears challenging, in spite of considerable progress in utilizing remote sensing data, increased spatial resolution, and the introduction of ensemble prediction methods. PLs can occasionally be forecasted to great perfection deterministically, while some are missed completely (e.g. Aspelien et al., 2011; Kristiansen et al., 2011). This is a serious situation is serious for the increased level of activities in some of the involved regions, and efforts should be made to reduce forecast failures.

1.2.   Mechanisms

Most of the updated knowledge about PLs 25-30 years after Wilhelmsen's (1985) description, is based on a few important observational campaigns involving well equipped aircrafts and on model studies. The gradually improved spatial resolution and representation of processes in NWP models, along with the exploitation of increasingly advances satellite data in data-assimilation, have also improved the situation for duty forecasters. The concepts for the development of PLs have thus developed considerably.

The "Norwegian polar low project (1983-85)" was an important effort to advance the conceptual understanding and the numerical forecasting of PLs (Lystad, 1986; Rasmussen and Lystad 1987). The project also provided the first comprehensive observations of a strong PL using aircraft (Shapiro et al., 1987). More than 20 years later the first full development of a PL from initial perturbation through its mature stages was covered by a series of flight campaigns in the Barents and the Norwegian Sea (Kristjánsson et al, 2011; Føre et al., 2011).

The knowledge gained from these and other studies has shown that PLs are not realizations of a single type of phenomenon. Already Lystad (1986) defined 4 different archetypes, and up to 7 types have later been defined (Rasmussen and Turner, 2003). PLs generally involve a trigger mechanism of dynamic instability in the lower troposphere for which an interaction between an upper-level potential vorticity anomaly and low-level baroclinicity is crucial (Hoskins et al., 1985).   Ruling out the relatively shallow and weak "comma clouds", the subsequent strengthening into PLs that extend to the Arctic tropopause depend on diabatic heating from latent heat by condensation. Føre et al. (2012) showed an example where exceptionally strong sensible heat fluxes close to the ice-edge was a crucial energy source for the growth phase.

The favorable environmental condition is a pronounced and sustained transport of extremely cold air over an ice-free ocean referred to as marine cold-air outbreaks (MCAOs). On satellite images it is customary to observe shallow to deep convective clouds aligned along the main wind direction. The initial baroclinic trigger is not believed to start from small random perturbations since the advection of an upper level positive potential vorticity anomaly across the low-level baroclinic zone from the cold to the warm side is required. The low-level baroclinicity can be associated with the ice-edge, the shallow Arctic front, or a remaining occlusion after a synoptic cyclone. In some regions, this frequently occurs with reversed shear flow when the thermal wind is directed opposite to the surface wind (Kolstad, 2006).

Two main proposals have been forwarded for the development phase, and both involve the organization of deep marine convection. Following the analogy with tropical cyclones, the conditional instability of the second kind (CISK) was proposed by Rasmussen (1979), and the potential of the mechanism was discussed by Bratseth (1985). The second mechanism is also an analogy to tropical cyclones and takes into account that there need not be any reservoir of convective available potential energy in the ambient atmosphere. It was proposed for PLs by Emanuel and Rotunno (1989) and termed wind-induced surface heat exchange (WISHE).

The recent study by Linders and Sætra (2010) indeed demonstrated that, based on advanced observations, PL development involving deep convection is possible without any reservoir of CAPE. From the data collected during the flight they found that any case with sizeable CAPE co-existed with unstable atmospheric boundary layers (ABL) over the ocean. CAPE was consistently close to zero when the ABL was stable. Situations with a conditionally unstable atmosphere were not detected, but rather that CAPE was consumed as it was produced with a time-scale of typically one hour. Their conclusion was that PL development does not require pre-existing CAPE. They also challenged the two-stage view of PL development with a baroclinic instability spin-up to be followed by intensification by e.g. WISHE, hypothesising that the processes may act in tandem.

For a very unique observationally based example of the trigger and development mechanisms for PLs in the Barents and Norwegian sea it is referred to Figures 7, 8, and 9 in Kristjansson et al. (2011) or Figures 2, 3, 4, and 10 in Føre et al (2010). In particular the vertical sections during the initial baroclinic phase shows a shallow baroclinic structure with a sharp low-level front, while that for the developed phase shows a deep equivalent-barotropic cyclonic vortex with a dry and warm core.

1.3. Flow Indices and Climatology

For duty weather forecasters it is traditionally important to monitor the large scale flow patterns over the areas that experience PLs. Awareness is increased when there are MCAO and the vertical temperature gradient is large, although the latter can be difficult to estimate from the very few radiosondes in the regions prone to PLs. Satellite imagery and numerical model products are therefore used as well, and Noer et al. (2011) made an updated 10-year climate statistics for 2000-2009 over the Nordic Sea based on the systematic monitoring by duty forecast meteorologists in Tromsø, Norway.

An increase from an average 7 cases per winter month identified by Wilhelmsen (1985) to 12 was found by Noer et al. (2011), who state that it is likely that this increase is at least partly artificial caused by the improved satellite and model data. Simplified indices employed by the forecasters on duty to diagnose reasons for increased awareness of PL occurrence, include

- Existence of a Major Cold Air Outbreak (MCAO)
- In a sub-area, SST – T(500hPa) > 43 °C
- Existence of upper-level trough, e.g. 500 hPa potential vorticity > 2 PVU

These elements are mainly based on output from high-resolution NWP-models which, according to subjective experience, can be unreliable for predicting the actual occurrence of PLs. Satellite images as well as scatterometer winds can help the forecaster to detect actual PLs during otherwise diagnosed favorable conditions. Additional features that need to be in place are the existence of a low-level baroclinic zone (old occlusions, shallow Arctic fronts), and the wind-speeds need to exceed gale force (15 m/s) in a resulting perturbation.

Kolstad (2011) performed and presented a climate statistics of PLs in any area during winter in both hemispheres. He used similar flow indices as defined above, although the static stability below 700 hPa was used rather than 500 hPa, and he used and an empirical database of 63 PLs to quantify the respective influences of low-level and upper-level forcing on PL formation. Based on threshold values for parameters characterizing the two features, statistics for favorable conditions for PL occurrence were presented the North Atlantic, the North-West Pacific and the Southern Hemisphere. One conclusion was that MCAOs puts important constraints on where PLs *can* form, while the upper-level forcing determines whether or not they *will* form.

The study concluded that major regions of occurrence from November through March are the Labrador Sea (up 14% of the time in February) and the Nordic and Barents Seas (up to 9% in December and January). In the North-West Pacific the maximum occurrence was diagnosed in the northern parts of the Japan Sea and to the east of northern Japan over the Kuroshio current (up to 12% in January) and over the Sea of Okhotsk to the west of Kamchatka (up to 10% in February). In the Southern Hemisphere, favorable conditions was found to occur substantially less frequent (up to 2-2.5% in July-August) and spread over two considerably larger regions to the south of New Zealand and to the north of the Amundsen Sea. In the preliminary numerical forecast verification below we focus on the NH winter 2012-13.

1.4.   Polar Lows and Climate Change

As the occurrence of PLs is associated with strong horizontal contrasts between ice-covered and ice-free sea during the extended winter season, any long-term changes in the Arctic sea-ice conditions due to global climate change will also impact the climatology of PLs. The main long-term reduction in Arctic sea-ice cover occurs in summer and fall and not in winter-spring. The properties of the sea-ice may change, however, when multi-year ice gradually is replaced by thinner and more homogenous ice generated during the same season. Even if this may reduce the temperature contrasts, it is not obvious to what extent the PL occurrence may change significantly, although a PL was observed for the first time north of Spitsbergen on January 8, 2010 (see Figure 2).

Kolstad and Bracegirdle (2008) analysed trends in MCAOs under scenarios for future climate change. They used output of sea-surface potential temperature and the 700 hPa potential temperature from global climate models contributing to the 4th assessment report (AR4) from the Intergovernmental Panel on Climate Change (IPCC). One problem with studies such as this is the bias in simulations of sea ice in the Barents Sea in most of the AR4 models. The largest projected weakening of MCAOs was estimated over the Labrador Sea, while over the Nordic Seas, the main region of strong MCAOs was estimated to move north and weaken slightly. Over the Sea of Japan, only a small weakening of MCAOs was projected.

Figure 2: Infrared satellite picture valid at 8.01.2003 11:27 UTC (NOAA-15), depicting a polar low north of Spitsbergen.

Zahn and von Storch (2010) based a future projection of PL occurrence on regionally downscaled IPCC AR4 models which thus enabled direct identification of PLs in the North Atlantic. No systematic change in PL frequency was found by Zahn and von Storch (2008) from a similar analysis re-analysis data (NCEP) from 1948 to 2005. From the downscaled projections towards the 21 century they estimated a significant reduction in North Atlantic PL occurrence along with a northward shift of the region where they are triggered and developed. They found that the main reason for the modelled change is a faster increase in the mid-tropospheric temperature than the SST, thus increasing the tropospheric static stability and suppressing the deep convection and release of latent heat. As these convective processes as well as the sea-ice must be considered uncertain, more elaborate model experiments are needed to further elaborate these first studies on climate change and PL occurrence.
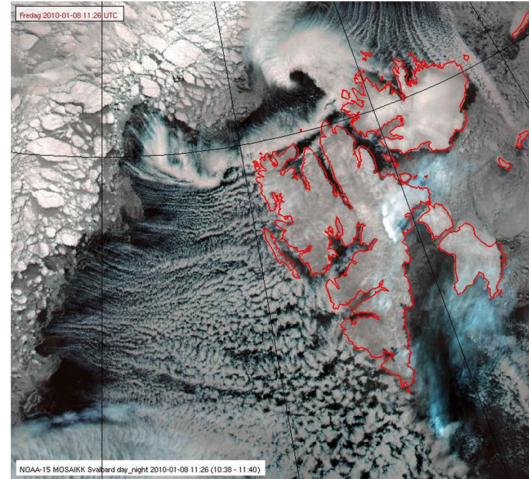
2.   Examples: NWP Forecast Verification

There several important factors that limit the predictability of PLs. The resolution of sharp contrasts in surface temperature is obviously limited if the mesh-width in the models is too coarse. This may also be influenced by the SST-distribution and the heat-conduction properties if the modelled sea-ice. Topography close to the region of interest also need to be adequately resolved, and the properties of the unstable, windy, marine ABL providing vertical fluxes of heat and water vapour require sufficient vertical resolution in the ABL.

For the growth and development of PLs into deep vortices, deep convection needs to be either explicitly modelled or parameterized well. The vertical profile of released latent heat of condensation is an important moderator of the efficiency of the spin-up of the PL (e.g. Bratseth, 1985). The release of available potential energy due to baroclinic instability may also be important during the growth and development phase acting in concert with the processes causing latent heat release. Furthermore, there may be important constructive feedbacks as PLs influence the mixing of water in the relatively shallow upper ocean. Relatively warm water may be mixed to the sea surface due to stirring of the well mixed water by the strong winds around a PL. The importance of this is not known since there is no operational NWP-model with sufficient resolution which is run fully coupled to the ocean.

Initial state uncertainty in the determination of the initial position of the upper level anomaly is evidently important. The same applies to low-level baroclinic features that are only weakly associated with geographically fixed contrasts. The paucity of regular observations, in particular in the free troposphere, is important in this connection, even though advanced data-assimilation of satellite data can help.

The latter was demonstrated by Randriamampianina et al. (2011) for the IPY Thorpex campaign period in the Norwegian Arctic from 25.02-17.03.2013 using the hydrostatic Aladin limited-area model with horizontal resolution ~11km, and 3D-Var data-assimilation with or without extra campaign in-situ data and with or without IASI satellite data (IASI=Infrared Atmospheric Sounding Interferometer). A clear positive impact of the IASI was seen for forecasts of the geo-potential in the mid-troposphere. Smaller but significant positive impacts were also found for the temperature and humidity in the lower troposphere.

Randriamampianina et al. (2011) also re-visited a particularly problematic case with a PL off the North-West coast of Norway on 16.03.08 12-18 UTC. The forecasts with the Norwegian operational limited-area ensemble prediction system had been particularly bad, and adding in-situ campaign observations actually worsened the forecast (Aspelien, 2011). Employing IASI-data, however, improved the forecast significantly. The improvement lasted up to 24 hours when the campaign data were excluded, and up to 36 hours when they were assimilated together with the IASI data.

2.1.   The Medium Range: ECMWF

The so-called high-resolution, deterministic forecasts produced operationally at ECMWF during 1.11.2012 through 30.03.2013 are here investigated. The horizontal resolution was approximately 16 km ($T_L 1279$) and there were 91 levels in the vertical. This resolution should enable explicit representation of PLs with radius larger than 100 km, provided the parameterization of deep convection and vertical fluxes of momentum, heat, and humidity in the extremely unstable marine boundary layer is reliable. However, as there is no software for detection and tracking of PLs available, we choose to verify the occurrence of events of MCAOs combined with gale force winds or stronger, defined as:

$$(SST - T500 > 43K) \ and \ (ff10 > 15m/s),\qquad\qquad(1)$$

where SST is the sea-surface temperature, T_{500} is the temperature at 500 hPa, and ff_{10} is the wind speed at 10m above ground. Although (1) is inspired by the criteria used by duty forecasters after several decades of experience, due to the omitted condition for a PV anomaly the selected events may include situations which would not be associated with PLs, or PLs may be erroneously neglected.

Figure 3 shows maps of analysed frequency of occurrence of these conditions in the Nordic Seas and in the North-West Pacific, along with 3-day forecasts made twice per day of the same. The period is the winter season November-March 2012-13. The spatial patterns are remarkably similar, although there are also considerable relative differences in the amplitudes of the frequency of occurrence, indicating that forecast errors are pronounced on a case-to-case basis. Verification of the individual forecasts of the over the season is made as a function of up-scaling radius of the forecast as well as the verifying analysis. Ideally verification should be made relative to independent observations and not the analysis which is a product of the same model that provides the forecast. Given the sparse regular

observation networks, such an ideal situation is not available in practice, however, and the raw satellite information is not suitable for direct verification. The up-scaling also requires the data to be available on a comparable grid as the forecasts.
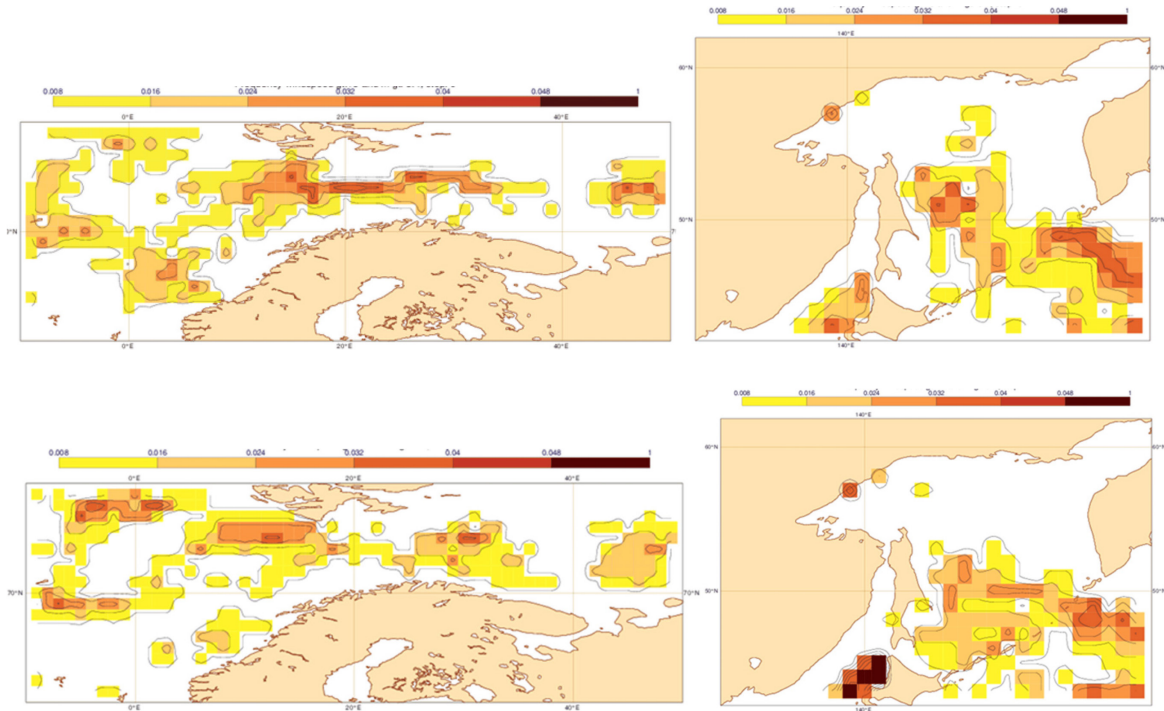

Figure 3: Frequency of the combined occurrence of (SST-T$_{500}$>43K) and (ff$_{10}$>15m/s) in the Nordic Seas (left column) and the North-West Pacific (right column) diagnosed from operational ECMWF analyses (upper row) and 3-day forecasts (lower row) during the winter 1.11.2012 – 30.03.2013.Isolines for 0.8, 1.6, 2.4, 3.2, 4.0 and 4.8 % of the time.

One may argue that there may be cases where the analysis may not be significantly better than the forecast given the few observations, in particular in cases which are particularly badly forecasted, since the analysis itself is part of the reason for the bad forecast. This is probably correct early in the development of the problematic feature (say 6-12 hours). Later, however, the amplitude of the fast developing feature is considerably larger and should be detected by satellite radiances if not by regular in situ observations. Here we define the forecasted (M) and analysed (O) probability of occurrence of the events selected by eq. (1) in any grid point as the fraction of neighbouring grid points (including itself), inside a circle of radius R around the grid point, where (1) is fulfilled. This procedure is called up-scaling and is a slight generalization of the proposed method by Roberts and Lean (2008) for precipitation for which dense networks of observations are available. For a given neighbourhood radius R the mean square error (MSE) of the M compared to O over all grid-points in a verification domain is defined, and the fractions skill score (FSS) is

$$FSS = 1 - \frac{MSE}{MSE_{ref}} \qquad (2)$$

where MSE$_{ref}$ is the mean square error of a reference forecast without any correlation between M and O. Hence, MSE$_{ref}$ is the largest possible MSE that can be obtained from the forecast and observed

fractions. As discussed by Roberts and Lean (2008) smaller FSS values than ca. 0.5 signify that the forecast has smaller skill than forecasting a uniform probability field equal to the fraction of the area covered by the event relative to the total area of the domain. Furthermore, as R increases a further increase of FSS will level off asymptotically to 1 (provided no forecast bias compare to the analyses), meaning that events will occur anywhere inside large circles. Hence, FSS-curves may help defining the smallest skillful spatial scales (FSS>0.5) and the largest useful scales (dFSS/dR approaching
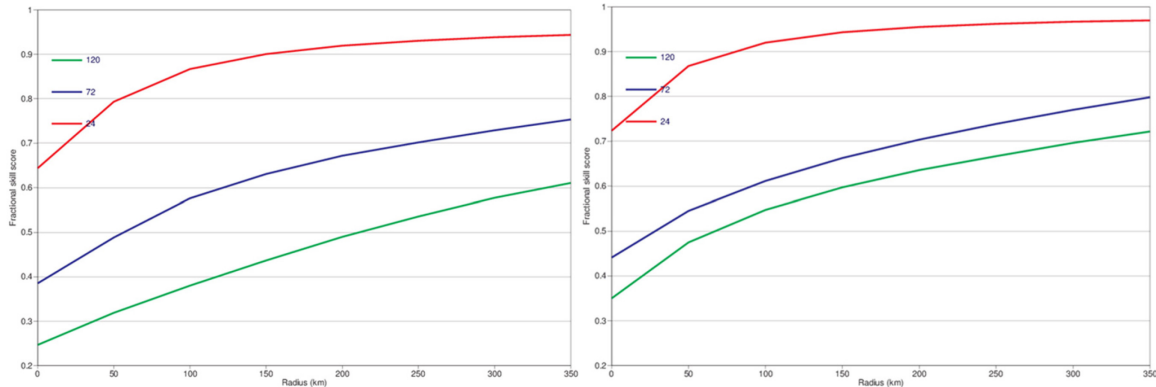

Figure 4: Fractions skill score as a function of upscale radius for the forecasted combined events (SST-T_{500}>43K) and (ff_{10}>15m/s) with the ECMWF T_L1279 model for the Nordic Seas (left) and the North-West Pacific (right) during 1.11.2012 through 30.03.2013. Red: 1day, blue: 3day, and green: 5day forecasts.

zero).

Figure 4 shows FSS for the event defined in eq. (1) for the ECMWF deterministic model for the winter 2012-2013. The one-day forecasts are skillful relative to a spatially uniform probability forecast for any value of R, but its usefulness quickly deteriorates beyond ca. 100 km radius, and perhaps even for shorter scales in the North-West Pacific. The three-day forecasts are skillful for R>~50(35) km and the five-day forecasts for R>~200(70) km for the Nordic Seas (North-West Pacific). The range of usefulness for large R is larger than for the one-day forecasts, but it is difficult to define a strict limit. Judging from the FSS in this particular season, the predictability of the event appears larger in the North-West Pacific than in the Nordic Seas.

2.2. The Short Range: GLAMEPS

The Grand limited-area model ensemble prediction system (GLAMEPS) developed by HIRLAM and some ALADIN countries in Europe is nested into the ECMWF ensemble system (ENS). It is described by Iversen et al. (2011) along with extensive verification
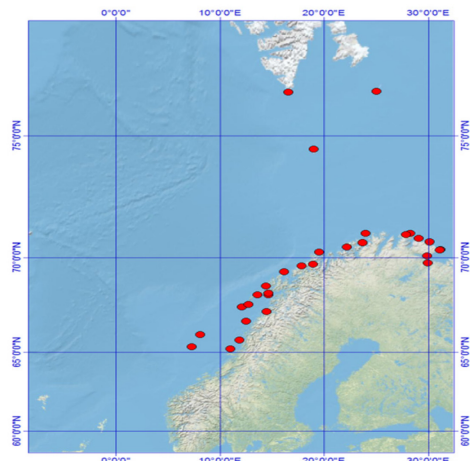

Figure 5: A selection of observational sites used for the verification of GLAMEPS forecasts presented below for the period 1.10.2012 – 15.04.2013.

using standard verification scores for probabilistic forecasts. Three different atmospheric analyses with three different models / model versions are part of the ensemble, and there are 36 different analyses of the ground surface properties. Otherwise, the spread amongst ensemble members are defined by the EC ENS data imposed at the lateral boundaries and for a subsection of ensemble members. The number of ensemble members is 54 and the system is run twice daily up to 54 hours with ~10km grid resolution.

Figure 5 shows the selected observation points used for verifying the daily GLAMEPS forecasts made from 06 UTC between 1st October 2012 and 15th April 2013. The events verified here are defined based on 10-meter wind speed. The GLAMEPS verification is compared to that issued by ECMWF (EC ENS) based on analyses at 00 UTC.

Figure 6 shows that the mean 10 m wind speed bias for GLAMEPS is smaller than EC ENS, and that GLAMEPS slightly under-estimates while EC ENS over-estimates. The figure also shows the ensemble spread and the RMS error for the ensemble mean. The under-estimated spread is smaller for GLAMEPS than for EC ENS, both because errors are smaller and the spread larger.

The continuous rank probability score (CRPS) for 10m wind speed is also included. CRPS is the integral over all possible event thresholds for the variable (here 10m wind speed) of the squared difference between the cumulative probability density functions (cdf) for the forecast and the verifying observation. The observation cdf reduces to a heavy-side step-function with the step from 0 to 1 at the observed value. CRPS ranges from zero for perfect forecasts to (theoretically) infinity. If the forecast is deterministic, the forecast cdf also reduces to a heavy-side step function, and CRPS becomes the mean absolute error (MAE). The lower diagram in Figure 6 shows clearly lower CRPS values for GLAMEPS than for EC ENS. The slight increase in CRPS with forecast length for GLAMEPS is not present for EC ENS, which may be taken as an indication that GLAMEPS improves the predictability for wind speed at the selected sites.
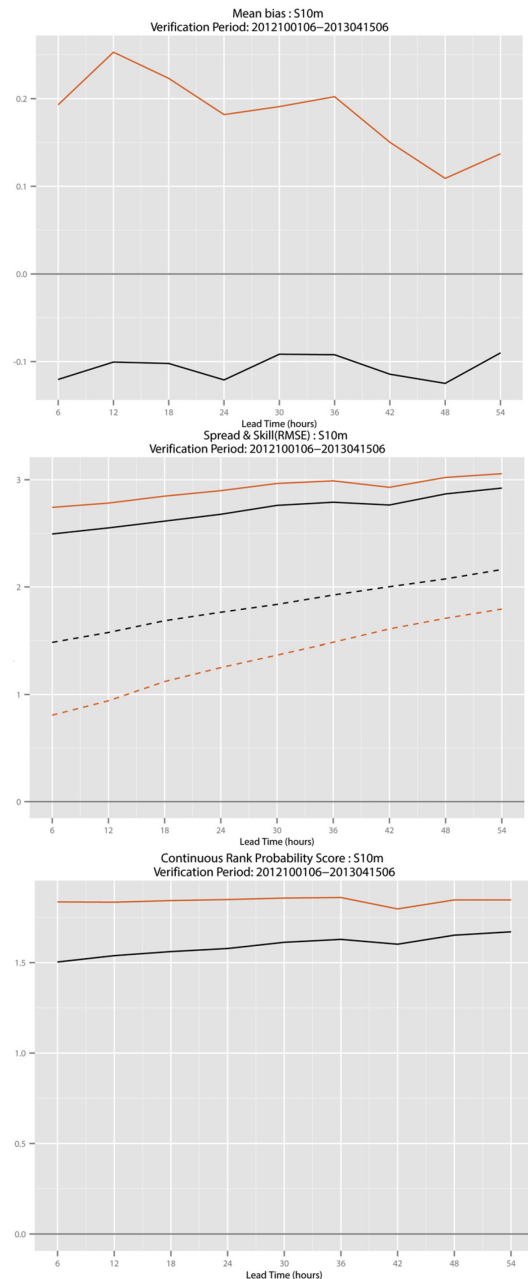

Figure 6: Three selected statistics for probabilistic verification of 10m wind speed as a function of forecast length. Black curves: GLAMEPS; red curves: EC ENS. Upper: Mean bias. Middle: RMS error (continuous) and RMS spread (dashed). Lower: Continuous Rank Probability Score (CRPS). All units: m/s.

Figure 7 shows a small selection of verification plots for 42h forecasts for event thresholds defined for 10 m wind speed. The reliability diagram for events of wind speeds exceeding 15 m/s clearly indicates too few data for stable statistics. We therefore concentrate our attention to the threshold 10 m/s, even though this event may occur frequently during winter at these coastal sites, without any occurrence of PLs. Unfortunately, the observations are only surface data and are insufficient for observing the status of any MCAO. Further verification targeted to PLs would either require vertical soundings or verification against analysed fields.
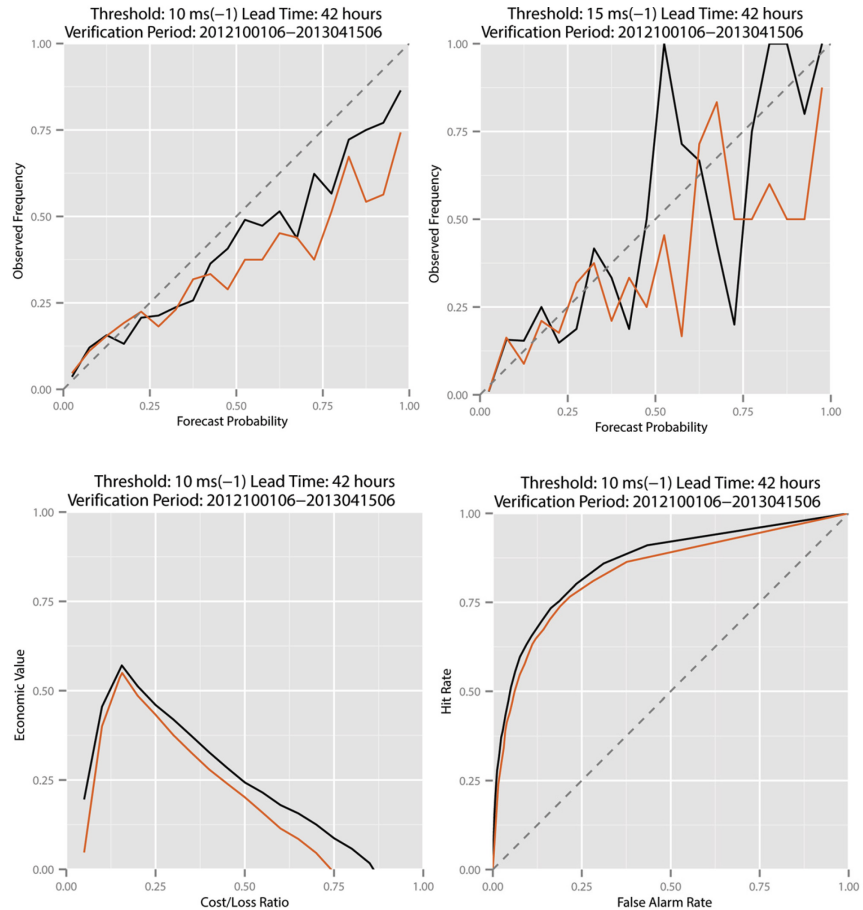
Nevertheless, for a wind speed threshold of 10

Figure 7: Upper row: Reliability diagrams for 42h forecasts of 10 m wind speed to exceed 10 m/s (left) and 15 m/s (right). Lower row: Expected value of the 42h forecasted 10 m wind speed to exceed 10 m/s as a function of the user's cost-loss ratio (left) and corresponding diagram for hit rate vs. false alarm rate (ROC-diagram). Black curves: GLAMEPS; red curves: EC ENS.

m/s, decisions made based on GLAMEPS should give more value for arbitrary user profiles, and the hit rates are increased while false alarm rates are reduced. Although data for several seasons would be necessary to verify higher wind thresholds, all the verification results are in consistent support of GLAMEPS with its higher resolution. The emphasis of GLAMEPS as a multi-model system data with and ensemble spread at low levels may also contribute to the improvement, although the SSTs are not perturbed in the present version of GLAMEPS (and neither in EC ENS).

2.3. Cloud-Permitting Forecasts: HarmonEPS

We will finally show an example of a convection-permitting model with non-hydrostatic dynamics and explicit deep moist convection: the HARMONIE model which employs the MeteoFrance AROME physical package. The horizontal resolution is 2.5 km and the number of layers in the vertical is 65. This system is intended to be set up with several pre-defined domains and to complete pure dynamical downscaling of coarse-resoltion ensemble forecasts, and is named HarmonEPS. In this case, 10 selected ensemble members and the control forecast of the operational EC ENS are used

as lateral boundary and initial conditions for 42h forecasts starting at 06 and 18 UTC. No data-assimilation is included.

Here we show some diagnostic results as strike probability maps for detected and tracked forecasted PLs in the Nordic Seas. The period is 23rd October 2012 to 22nd April 2013. The considerably smaller ensemble size (~20%) of HarmonEPS is partly the reason why the standard probabilistic verification have slightly poorer results for HarmonEPS than for GLAMEPS for the same coastal sites (Figure 5) in the Norwegian Arctic (graphics omitted here). Another reason is that HarmonEPS has a larger bias (~ - 0.5 m/s vs. ~ - 0.1 m/s) for 10 m wind speed. The smaller ensemble size results in reduced ensemble spread, and since the RMS error is comparable to GLAMEPS, the HarmonEPS ensemble spread exaggerates the estimated quality of the ensemble mean for 10 m wind speed on these sites.
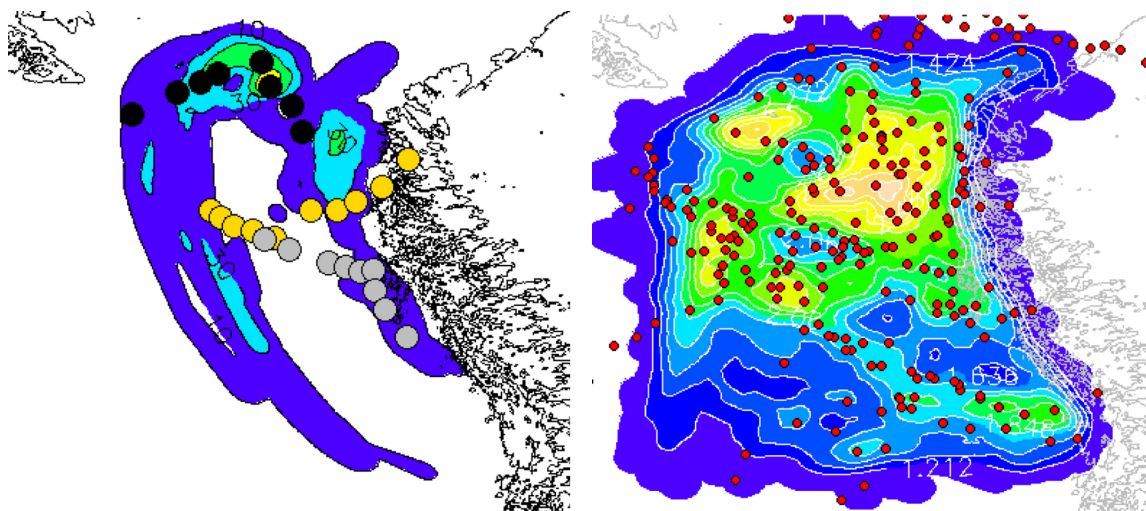

Figure 8: Estimated probabilities for a polar low to strike a grid square of size 2.5kmx2.5kmbased on the HarmonEPS dynamical downscaling of 10 ensemble members and the control forecast from EC ENS. Circles / dots are verifying polar low positions during the forecast period subjectively identified by the duty forecaster in Tromsø, Norway. Left: Forecast strike probability map for 24.10.12 06+42h. The dots with different colours indicate different polar lows. Right: average strike probabilities for the entire period 23.10.12 to 22.04.13. Red dots are subjectively diagnosed polar lows by the duty forecaster in Tromsø, Norway. Notice that the red dots close to the upper border are close to and partly outside the border of the integration domain for HarmonEPS.

For the time being we therefore regard the present version of HarmonEPS as a system for interpretation of EC ENS on selected small regions. In the winter half of the year, the system downscales EC ENS for the purpose of detecting and tracking PLs up to 42h in advance, based on a further elaborated tracking algorithm described by Kristiansen et al. (2011). Figure 8 shows an example of a strike probability map for three PLs, along with a map of probabilities for the entire winter season. The duty forecasters in Tromsø, Norway make use of the strike probability maps under situations when the large scale atmospheric circulation provide conditions for PL development. Work is underway to evaluate the quality and reliability more objectively using standard probabilistic verification on the forecasted strike probabilities.

3. Concluding Remarks

We have presented and discussed several aspects of NWP based forecasts of polar lows. It is clearly possible to forecast PLs up to a few days ahead using probabilistic techniques. At the same time, complete failures are also possible.

The objective verification presented here evaluate variables and probabilities of events based on given thresholds which are only indirectly associated with PLs. Some of them are not specifically associated with only PLs, and the verification thus evaluate other features than PLs. This is a consequence of the paucity of three-dimensional atmospheric observations in the region where PLs occur. Work is on-going to better identify and verify events that are more closely associated with PLs, such as the strike probability maps produced after downscaling of coarser resolution ensembles.

It is already well recognized that PLs develop very quickly under favourable conditions. Sparse observation networks may directly cause serious forecast failures when positions of upper-level troughs and low level baroclinic zones at initial time are missing or wrong. Utilizing advanced satellite date (e.g. IASI) can reduce the number of failures, but the value of such data is increased when the availability of regular in situ data are enhanced simultaneously.

References

Aspelien, T., T. Iversen, J. B. Bremnes, and I.-L. Frogner, 2011: Short-range probabilistic forecasts from the Norwegian limited-area EPS: Long-term validation and a polar low study. *Tellus,* **63A,** 564–584.

Bratseth, A. M. 1985. A note on CISK in polar air masses. *Tellus* **37A**, 403–406.

Emanuel, K. A. and Rotunno, R. 1989. Polar lows as arctic hurricanes. *Tellus* **49A**, 1–17.

Føre, I., J. E. Kristjánsson, Ø. Saetra, Ø. Breivik, B. Røsting, and M. Shapiro, 2011: The full life cycle of a polar low over the Norwegian Sea observed by three research aircraft flights. *Quart. J. Roy. Meteor. Soc.,* **137**, 1659–1673. doi:10.1002/qj.825.

Føre I, Kristjansson JE, Kolstad EW, Bracegirdle TJ, Saetra Ø, Røsting B. 2012. A 'hurricane-like' polar low fuelled by sensible heat flux: high-resolution numerical simulations. *Q. J. R. Meteorol. Soc.* **138**, 1308–1324. DOI:10.1002/qj.1876

Hoskins, B. J., M. E. McIntyre, and A. W. Robertson, 1985: On the significance of isentropic potential vorticity maps. *Quart. J. Roy. Meteor. Soc.,* **111,** 877–946.

Iversen, T., Deckmyn, A., Santos, C., Sattler, K., Bremnes, J. B., Feddersen, H., and Frogner, I.-L., 2011. Evaluation of 'GLAMEPS'—a proposed multimodel EPS for short range forecasting. *Tellus,* **63A,** 513–530. doi: 10.1111/j.1600-0870.2010.00507.x

Kolstad, E. W. 2006. A new climatology of favourable conditions for reverse-shear polar lows. *Tellus* **58A**, 344–354.

Kolstad, E. W. 2011. A global climatology of favourable conditions for polar lows. *Q. J. R. Meteorol. Soc.* **137**: 1749–1761. DOI:10.1002/qj.888

Kolstad, E. W. and T. J. Bracegirdle (2008): Marine cold-air outbreaks in the future: an assessment of IPCC AR4 model results for the northern hemisphere. *Climate Dynamics*, 30(7–8): 871-885. DOI: 10.1007/s00382-007-0331-0.

Kristiansen, J., Sørland, S. L., Iversen, T., Bjørge, D. and Køltzow, M.Ø. 2011. High-resolution ensemble prediction of a polar low development. *Tellus* **63A**, 585–604.

Kristjansson, J. E., Barstad, I., Aspelien, T., Føre, I., Godøy, Ø. A., Hov, Ø., Irvine, E., Iversen,T., Kolstad, E. W., Nordeng, T. E., McInnes, H., Randriamampianina, R., Reuder, J., Sætra, Ø., Shapiro, M. A., Spengler, T., Ólafsson, H., 2011: The Norwegian IPY-THORPEX. Polar Lows and Arctic Fronts during the 2008 Andøya Campaign. *Bulletin of The American Meteorological Society - (BAMS).* ISSN 0003-0007. *92*(11), s 1443- 1466 . doi: 10.1175/2011BAMS2901.1

Linders, T. and Sætra, Ø. 2010. Can Cape Maintain Polar Lows?. *J. Atmos. Sci.* **67**(8), 2559–2571 doi:10.1175/2010JAS3131.1.

Lystad, M., 1986, *'Polar Lows in the Norwegian Greenland and Barents Sea'*, Polar Lows Project, Final Report. The Norwegian Meteorological Institute: Oslo, Norway; 196 pp.

Noer G, Saetra Ø, Lien T, Gusdal Y. 2011. A climatological study of polar lows in the Nordic Seas. *Q. J. R. Meteorol. Soc.,* **137**, 1762–1772. DOI:10.1002/qj.846

Økland, H. 1977. On the intensification of small-scale cyclones formed in very cold air masses heated by the ocean. *Institute Report Series* **26**, University of Oslo, Department of Geophysics.

Rabbe, Å. 1975. Arctic instability lows. *Meteorologiske Annaler* **6**, 303–329.

Randriamampianina R, Iversen T, Storto A. 2011. Exploring the assimilation of IASI radiances in forecasting polar lows. *Q. J. R. Meteorol. Soc.* **137**: 1700–1715. DOI:10.1002/qj.838

Rasmussen, E., 1979: The polar low as an extratropical CISK disturbance. *Quart. J. Roy. Meteor. Soc.,* **105,** 541–549.

Rasmussen, E. and M. Lystad, 1987: The Norwegian polar lows project: a summary of the international conference on polar lows. *Bull. Amer. Meteor. Soc.*, **68**, 801–816.

Rasmussen, E. A. and J. Turner, 2003: *Polar Lows: Mesoscale Weather Systems in the Polar Regions.* Cambridge University Press, 612 pp.

Roberts, Nigel M., Humphrey W. Lean, 2008: Scale-Selective Verification of Rainfall Accumulations from High-Resolution Forecasts of Convective Events. *Mon. Wea. Rev.*, **136**, 78–97. doi: 10.1175/2007MWR2123.1

Shapiro, M. A., L. S. Fedor, and T. Hampel, 1987: Research aircraft measurements of a polar low over the Norwegian Sea. *Tellus*, **39A**, 272–306.

Wilhelmsen K. 1985. Climatological study of gale-producing polar lows near Norway. *Tellus,* **37A**, 451–459.

Zahn.M. and von Storch, H. 2008, A long-term climatology of North Atlantic polar lows. *Geophys. Res. Lett.,* **35**, L22702.

Zahn, M. and von Storch, H. 2010, Decreased frequency of North Atlantic polar lows associated with future climate warming. *Nature*, **467**, 309-312. DOI:10.1038/nature09388